Journal of Sound and Vibration (1997) **204**(1), 1–16

VIBRATION ANALYSIS OF RECTANGULAR MINDLIN PLATES RESTING ON ELASTIC EDGE SUPPORTS

Y. XIANG

School of Civil and Environmental Engineering, The University of Western Sydney Nepean, Kingswood, NSW 2747, *Australia*

K. M. LIEW

School of Mechanical and Production Engineering, Nanyang Technological University, Singapore 639798

AND

S. KITIPORNCHAI

Department of Civil Engineering, The University of Queensland, Brisbane, QLD 4072, *Australia*

(*Received* 3 *October* 1995; *and in final form* 11 *January* 1996)

For the first time to the authors' knowledge, the problem of free vibration of a moderately thick rectangular plate with edges elastically restrained against transverse and rotational displacements is considered. The Ritz method combined with a variational formulation and Mindlin plate theory is used. The admissible functions consist of polynomials and basic functions that impose the required boundary conditions on the Mindlin plate. The applicability of the formulation is illustrated using three examples of plates with different combinations of elastically restrained edges and classical boundary conditions. Numerical results are obtained to investigate the effects of elastic spring stiffness, relative thickness and aspect ratio upon the natural frequencies of flexural vibration of rectangular Mindlin plates.

1. INTRODUCTION

The vibration of rectangular plates with classical boundary conditions [1–4] and elastically restrained edges [5–18] has been widely analysed over the past few decades. Researchers have drawn attention to the latter problem because it is generally accepted that edge supports of a plate are elastic. Most interest is derived from potential practical application to industrial problems such as vibrations encountered in building construction, printed circuit boards, marine and aircraft structures. The excellent reviews of Leissa [19–21] have summarized most of the related work existing in open literature. From these reviews, the authors found that most work had been based on classical thin plate theory (CTPT). Limitations of the CTPT [22], however, have limited the application of the thin plate results to thick plate design although thick plates are important structural elements in many engineering applications. Chung *et al*. [14] studied the vibration of orthotropic Mindlin plates with edges elastically restrained against rotation. No results have been found in open literature for vibration of thick plates with edges elastically restrained against both transverse and rotational displacements. Prompted by the lack of research work in this

0022–460X/97/260001 + 16 $25.00/0/sv960922

area, this paper aims to provide some vibration solutions for thick plates with elastic edge supports.

In this study, the authors have employed the first order theory of Mindlin [22] to incorporate the effects of transverse shear deformation and rotary inertia on the vibration behaviour of thick plates. The integral expressions for the displacement-based strain and kinetic energy functional have been derived according to Mindlin plate theory [22]. Elastic edge restraints have been imposed by placing a set of springs along the plate edges that provide elastic support in both the transverse and rotational directions of the plate. In the numerical process, the transverse displacement and rotation fields have been approximated by sets of Ritz functions which are associated with the geometric boundary conditions implicitly and thus satisfy the geometric boundary constraints at the outset. Following the Ritz procedure with the integral expressions of the displacement-based strain and kinetic energy functional, and the Ritz functions, the governing eigenvalue equation has been derived. The paper describes details of the analysis method and formulations for the free vibration of Mindlin plates with elastically restrained edges.

Numerical results in terms of vibration frequency parameters for rectangular Mindlin paltes of various combinations of classical and elastically restrained boundary conditions are presented. The problems considered herein include plates with (1) four edges elastically restrained against rotational and transverse displacement, (2) two opposite edges simply supported and the others elastically restrained, and (3) two opposite edges clamped and the others elastically restrained. The effects of plate aspect ratio, relative thickness ratio and elastic spring stiffness parameters upon the vibratory behaviour of Mindlin plates are examined. Frequency parameters for plates with elastically supported edges are compared with the results available in the literature and found to be in excellent agreement.

2. GOVERNING EIGENVALUE EQUATIONS

Consider a flat, isotropic and moderately thick rectangular plate with uniform thickness t, length a, width b, elastic modulus E, shear modulus $G = E/[2(1 + v)]$ and Poisson ratio v (see Figure 1). The plate can have any combination of edge conditions and may be elastically restrained against lateral deflection and rotations on prescribed edges. The objective of the study is to determine the natural frequencies of the plate with elastically restrained edges.

For free harmonic vibration of a plate, the maximum strain energy functional based on the Mindlin shear deformation plate theory [22] can be expressed as:

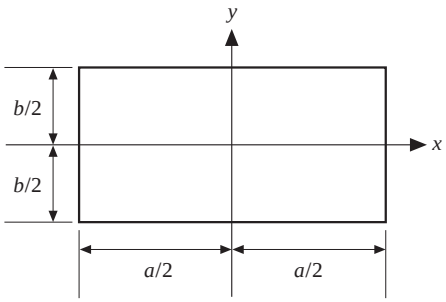

Figure 1. Geometry and co-ordinate system of rectangular plate analysed.

$$U = \frac{1}{2}\int_V \left\{ \frac{Ez^2}{1-v^2}\left[\left(\frac{\partial \theta_x}{\partial x} + \frac{\partial \theta_y}{\partial y} \right)^2 - 2(1-v)\left(\frac{\partial \theta_x}{\partial x}\frac{\partial \theta_y}{\partial y} - \frac{1}{4}\left(\frac{\partial \theta_x}{\partial y} + \frac{\partial \theta_y}{\partial x} \right)^2 \right) \right] \right.$$

$$\left. + \kappa G\left[\left(\theta_x + \frac{\partial w}{\partial x} \right)^2 + \left(\theta_y + \frac{\partial w}{\partial y} \right)^2 \right] \right\} \mathrm{d}V, \tag{1}$$

where V is the volume of the plate, z is the co-ordinate out of the plate plane, w is the lateral deflection on the midplane of the plate, θ_x and θ_y are rotations of the plate along the y and x directions, and κ is the shear correction factor associated with the Mindlin plate theory.

Note that if $\theta_x = -\partial w/\partial x$ and $\theta_y = -\partial w/\partial y$, equation (1) reduces to the well-known energy functional for thin plates.

The maximum kinetic energy of a Mindlin plate, T, can be derived as

$$T = \tfrac{1}{2}\omega^2 \int_A [\rho t w^2 + \tfrac{1}{12}\rho t^3(\theta_x^2 + \theta_y^2)]\, \mathrm{d}A, \tag{2}$$

in which ρ is the plate density per unit volume; ω is angular frequency; A is the area of the plate; and t is the thickness of the plate.

It is assumed that the stiffness of the elastic restraint for the lateral deflection is k_w and the stiffness for the rotational restraint is k_ϕ. If an edge has an elastic rotational restraint, only the rotation along the edge has been restrained in this study. The maximum strain energy stored by the elastic edge restraints can be expressed as

$$U_s = \frac{\delta_1}{2}\int_{-a/2}^{a/2} k_w [w|_{y=-b/2}]^2\, \mathrm{d}x + \frac{\delta_2}{2}\int_{-a/2}^{a/2} k_w [w|_{y=b/2}]^2\, \mathrm{d}x$$

$$+ \frac{\delta_3}{2}\int_{-b/2}^{b/2} k_w [w|_{x=-a/2}]^2\, \mathrm{d}y + \frac{\delta_4}{2}\int_{-b/2}^{b/2} k_w [w|_{x=a/2}]^2\, \mathrm{d}y$$

$$+ \frac{\delta_5}{2}\int_{-a/2}^{a/2} k_\phi [\theta_y|_{y=-b/2}]^2\, \mathrm{d}x + \frac{\delta_6}{2}\int_{-a/2}^{a/2} k_\phi [\theta_y|_{y=b/2}]^2\, \mathrm{d}x$$

$$+ \frac{\delta_7}{2}\int_{-b/2}^{b/2} k_\phi [\theta_x|_{x=-a/2}]^2\, \mathrm{d}y + \frac{\delta_8}{2}\int_{-b/2}^{b/2} k_\phi [\theta_x|_{x=a/2}]^2\, \mathrm{d}y, \tag{3}$$

in which δ_i, $i = 1, 2, \ldots, 8$, are the switch parameters. When $\delta_i = 0$, the ith restraint on the edge is removed; when $\delta_i = 1$, the ith restraint on the edge is imposed.

For generality and convenience, the global co-ordinates may be normalised with respect to the plate dimensions, i.e.,

$$\xi = x/a; \quad \eta = y/b. \tag{4}$$

Using equation (4), the normalised maximum strain and kinetic energy functional for the Mindlin plate and the strain energy stored in the elastical restraints may be expressed as

$$U = \frac{1}{2}\int_{\bar{A}} \left\{ D\left[\left(\frac{1}{a}\frac{\partial \theta_x}{\partial \xi} + \frac{1}{b}\frac{\partial \theta_y}{\partial \eta} \right)^2 - 2(1-\nu)\left(\frac{1}{ab}\frac{\partial \theta_x}{\partial \xi}\frac{\partial \theta_y}{\partial \eta} - \frac{1}{4}\left(\frac{1}{b}\frac{\partial \theta_x}{\partial \eta} + \frac{1}{a}\frac{\partial \theta_y}{\partial \xi} \right)^2 \right) \right] \right.$$

$$\left. + \kappa G t\left[\left(\theta_x + \frac{1}{a}\frac{\partial w}{\partial \xi} \right)^2 + \left(\theta_y + \frac{1}{b}\frac{\partial w}{\partial \eta} \right)^2 \right] \right\} ab \, \mathrm{d}\bar{A}, \tag{5}$$

$$T = \tfrac{1}{2}\omega^2 \rho \int_{\bar{A}} [tw^2 + \tfrac{1}{12}t^3(\theta_x^2 + \theta_y^2)] ab \, \mathrm{d}\bar{A}, \tag{6}$$

$$U_s = \frac{\delta_1}{2}\int_{-1/2}^{1/2} k_w [w|_{\eta=-1/2}]^2 a \, \mathrm{d}\xi + \frac{\delta_2}{2}\int_{-1/2}^{1/2} k_w [w|_{\eta=1/2}]^2 a \, \mathrm{d}\xi$$

$$+ \frac{\delta_3}{2}\int_{-1/2}^{1/2} k_w [w|_{\xi=-1/2}]^2 b \, \mathrm{d}\eta + \frac{\delta_4}{2}\int_{-1/2}^{1/2} k_w [w|_{\xi=1/2}]^2 b \, \mathrm{d}\eta$$

$$+ \frac{\delta_5}{2}\int_{-1/2}^{1/2} k_\phi [\theta_y|_{\eta=-1/2}]^2 a \, \mathrm{d}\xi + \frac{\delta_6}{2}\int_{-1/2}^{1/2} k_\phi [\theta_y|_{\eta=1/2}]^2 a \, \mathrm{d}\xi$$

$$+ \frac{\delta_7}{2}\int_{-1/2}^{1/2} k_\phi [\theta_x|_{\xi=-1/2}]^2 b \, \mathrm{d}y + \frac{\delta_8}{2}\int_{-1/2}^{1/2} k_\phi [\theta_x|_{\xi=1/2}]^2 b \, \mathrm{d}y, \tag{7}$$

where $\bar{A}$ is the non-dimensional area of the plate; $\mathrm{d}\bar{A} = \mathrm{d}\xi \, \mathrm{d}\eta$; and D is the flexural rigidity of the plate $= Et^3/[12(1-\nu^2)]$.

After choosing a set of appropriate admissible functions for w, θ_x and θ_y, the eigenvalue equation can be derived by applying the Rayleigh–Ritz method to minimize the differences between the maximum strain energies [equations (5) and (7)] and the maximum kinetic energy [equation (6)]. A procedure for forming a set of trial functions which satisfy the geometric boundary conditions of Mindlin plates of arbitrary shapes has been proposed by the authors [23–25]. A brief description of the procedure is given below.

The transverse deflection, w, and the rotations, θ_x and θ_y may be parametrized by

$$w(\xi, \eta) = \sum_{q=0}^{p}\sum_{i=0}^{q} c_m \phi_m(\xi, \eta) = \mathbf{c}^{\mathrm{T}}\boldsymbol{\phi}, \tag{8a}$$

$$\theta_x(\xi, \eta) = \sum_{q=0}^{p}\sum_{i=0}^{q} d_m \psi_{xm}(\xi, \eta) = \mathbf{d}^{\mathrm{T}}\boldsymbol{\psi}_x, \tag{8b}$$

$$\theta_y(\xi, \eta) = \sum_{q=0}^{p}\sum_{i=0}^{q} e_m \psi_{ym}(\xi, \eta) = \mathbf{e}^{\mathrm{T}}\boldsymbol{\psi}_y, \tag{8c}$$

where p is the degree set of a mathematically complete polynomial; **c**, **d** and **e** are row matrices and their corresponding elements c_m, d_m and e_m are the unknown coefficients to be varied with the subscript m which is given by

$$m = (q + 1)(q + 2)/2 - i \tag{9}$$

and $\boldsymbol{\phi}$, $\boldsymbol{\psi}_x$ and $\boldsymbol{\psi}_y$ are row matrices with elements:

$$\phi_m(\xi, \eta) = (\xi^{q-i}\eta^i)\phi_1(\xi, \eta), \tag{10a}$$

$$\psi_{xm}(\xi, \eta) = (\xi^{q-i}\eta^i)\psi_{x1}(\xi, \eta), \tag{10b}$$

$$\psi_{ym}(\xi, \eta) = (\xi^{q-i}\eta^i)\psi_{y1}(\xi, \eta) \tag{10c}$$

in which ϕ_1, ψ_{x1} and ψ_{y1} are basic functions that must satisfy the geometric boundary conditions of Mindlin plates. The details of these geometric boundary conditions for Mindlin plates have been discussed previously by the authors [24, 25].

The basic functions perform a key role in making the trial functions satisfy the geometric boundary conditions of a Mindlin plate. They are formed by manipulating the piecewise boundary expressions of the plate.

The basic function for the transverse deflection, w, can be expressed as

$$\phi_1(\xi, \eta) = \prod_{j=1}^{4} [\Gamma_j(\xi, \eta)]^{\Omega_j}, \tag{11a}$$

where $\Gamma_j(\xi, \eta) = 0$ is the boundary equation of the jth supporting edge; and Ω_j, depending on the support edge condition, takes on:

$$\Omega_j = 0 \text{ if the } j\text{th edge is free (F);} \tag{11b}$$

$$\Omega_j = 1 \text{ if the } j\text{th edge is clamped (C), or simply supported (S).} \tag{11c}$$

The basic functions for the rotations, θ_x and θ_y, are given by:

$$\psi_{x1} = \prod_{j=1}^{4} [\Gamma_j(\xi, \eta)]^{\Omega_j}, \tag{12a}$$

while

$$\Omega_y = 0 \text{ if the } j\text{th edge is free (F) or simply supported (S) in the } y \text{ direction;} \tag{12b}$$

$$\Omega_j = 1 \text{ if the } j\text{th edge is clamped (C) or simple supported (S) in the } x \text{ direction.} \tag{12c}$$

and

$$\psi_{y1} = \prod_{j=1}^{4} [\Gamma_j(\xi, \eta)]^{\Omega_j} \tag{13a}$$

while

$$\Omega_j = 0 \text{ if the } j\text{th edge is free (F) or simply supported (S) in the } x \text{ direction;} \tag{13b}$$

$$\Omega_j = 1 \text{ if the } j\text{th edge is clamped (C) or simply supported (S) in the } y \text{ direction.} \tag{13c}$$

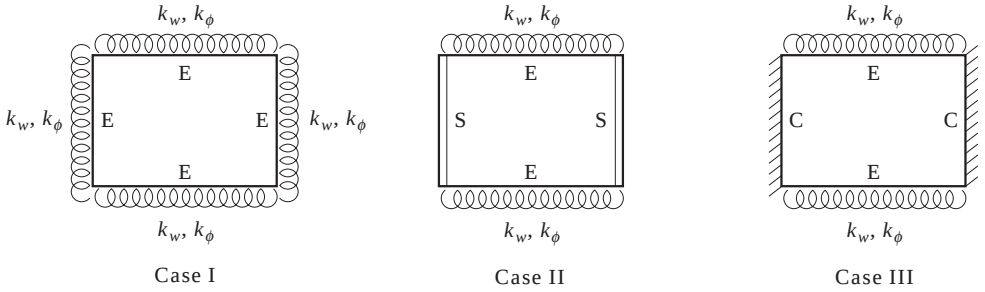

Figure 2. Rectangular plates with (I) four edges elastically restrained; (II) two edges simply supported and the other two edges restrained; and (III) two edges clamped and the other two edges elastically restrained.

Minimization of the differences between the maximum strain energies and kinetic energy of the Mindlin plate and the elastic edge restraints with respect to the unknown coefficients yields:

$$(\partial/\partial c_i)(U + U_s - T) = 0 \qquad i = 1, 2, \ldots, \bar{m}, \tag{14a}$$

$$(\partial/\partial d_i)(U + U_s - T) = 0 \qquad i = 1, 2, \ldots, \bar{m}, \tag{14b}$$

$$(\partial/\partial e_i)(U + U_s - T) = 0 \qquad i = 1, 2, \ldots, \bar{m}, \tag{14c}$$

which leads to

$$(\mathbf{K} + \mathbf{K}_s - \omega^2\mathbf{M})\begin{Bmatrix}\mathbf{c}\\ \mathbf{d}\\ \mathbf{e}\end{Bmatrix} = 0, \tag{15}$$

in which $\bar{m}$ is the total number of polynomial terms in (8) and can be determined by (9) with $i = 0$ and $q = p$. $\mathbf{K}$ and $\mathbf{M}$ are the stiffness and mass matrices of the plate and $\mathbf{K}_s$ is the stiffness matrix for the elastic edge restraints.

The matrices $\mathbf{K}$, $\mathbf{M}$ and $\mathbf{K}_s$ in equation (15) can be expressed in the form:

$$\mathbf{L} = \begin{bmatrix} \mathbf{L}_{cc} & \mathbf{L}_{cd} & \mathbf{L}_{ce} \\ & \mathbf{L}_{dd} & \mathbf{L}_{de} \\ \text{symm.} & & \mathbf{L}_{ee} \end{bmatrix} \tag{16}$$

in which $\mathbf{L}$ is replaced by $\mathbf{K}$, $\mathbf{M}$ or $\mathbf{K}_s$ as appropriate. The submatrices for the linear stiffness matrix of the Mindlin plate, $\mathbf{K}$, can be derived as:

$$\mathbf{K}_{cc} = \frac{\kappa G t}{ab}\int_{\bar{A}}\left(b^2\frac{\partial\boldsymbol{\phi}}{\partial\xi}\frac{\partial\boldsymbol{\phi}^{\mathrm{T}}}{\partial\xi} + a^2\frac{\partial\boldsymbol{\phi}}{\partial\eta}\frac{\partial\boldsymbol{\phi}^{\mathrm{T}}}{\partial\eta}\right)\mathrm{d}\bar{A}, \tag{17a}$$

$$\mathbf{K}_{cd} = b\kappa G t\int_{\bar{A}}\frac{\partial\boldsymbol{\phi}}{\partial\xi}\boldsymbol{\psi}_x^{\mathrm{T}}\,\mathrm{d}\bar{A}, \qquad \mathbf{K}_{ce} = a\kappa G t\int_{\bar{A}}\frac{\partial\boldsymbol{\phi}}{\partial\eta}\boldsymbol{\psi}_y^{\mathrm{T}}\,\mathrm{d}\bar{A}, \tag{17b, c}$$

$$\mathbf{K}_{dd} = \frac{D}{ab}\int_{\bar{A}}\left[b^2\frac{\partial\boldsymbol{\psi}_x}{\partial\xi}\frac{\partial\boldsymbol{\psi}_x^{\mathrm{T}}}{\partial\xi} + \frac{(1-\nu)a^2}{2}\frac{\partial\boldsymbol{\psi}_x}{\partial\eta}\frac{\partial\boldsymbol{\psi}_x^{\mathrm{T}}}{\partial\eta} + a^2b^2\kappa G t\boldsymbol{\psi}_x\boldsymbol{\psi}_x^{\mathrm{T}}\right]\mathrm{d}\bar{A}, \tag{17d}$$

TABLE 1

Convergence studies of frequency parameter, $\lambda = (\omega b^2/\pi^2)\sqrt{\rho t/D}$, *for square Mindlin plate with four edges elastically restrained* (EEEE *plate*, $a/b = 1$).

			Mode sequence								
$S_w = S_\phi$	t/b	p_s	1	2	3	4	5	6	7	8	9
10^2	0·001	4	1·7603	2·6949	2·6949	3·6183	4·8532	4·9552	20·6793	20·6793	28·6970
		6	1·7578	2·5719	2·5719	3·4376	4·6536	4·7325	6·2926	6·2926	10·0450
		8	1·7566	2·5604	2·5604	3·4319	4·6502	4·7136	5·7341	5·7341	8·4702
		10	1·7566	2·5599	2·5599	3·4317	4·6483	4·7135	5·7190	5·7190	8·4123
		12	1·7566	2·5599	2·5599	3·4317	4·6483	4·7135	5·7184	5·7184	8·4111
		13	1·7566	2·5599	2·5599	3·4317	4·6483	4·7135	5·7184	5·7184	8·4111
		14	1·7566	2·5599	2·5599	3·4317	4·6483	4·7135	5·7184	5·7184	8·4111
	0·20	4	1·6265	2·4265	2·4265	3·2797	4·0668	4·1667	6·7595	6·7595	10·4455
		6	1·6220	2·3774	2·3774	3·1341	3·9153	3·9858	4·7870	4·7870	6·6096
		8	1·6216	2·3760	2·3760	3·1282	3·9100	3·9774	4·6619	4·6619	6·1635
		10	1·6216	2·3760	2·3760	3·1281	3·9096	3·9773	4·6584	4·6584	6·1363
		12	1·6216	2·3760	2·3760	3·1281	3·9096	3·9773	4·6584	4·6584	6·1357
		13	1·6216	2·3760	2·3760	3·1281	3·9096	3·9773	4·6584	4·6584	6·1357
		14	1·6216	2·3760	2·3760	3·1281	3·9096	3·9773	4·6584	4·6584	6·1357
10^8	0·001	4	404·967	1216·646	1216·646	1806·153	1896·292	1921·437	4168·656	4168·656	5021·448
		6	111·9608	445·1614	445·1614	700·4806	887·4712	924·766	1912·863	1912·863	2223·955
		8	3·6475	118·0916	118·0916	166·4638	305·1889	328·3795	748·4753	748·4753	904·3638
		10	3·6476	7·5241	7·5263	11·0020	13·9042	14·0368	140·7839	140·7839	214·8212
		12	3·6464	7·4374	7·4400	10·9691	13·3629	13·4157	17·0995	7·0997	22·7086
		13	3·6476	7·4366	7·4367	10·9691	13·3619	13·4138	16·7379	6·7380	21·4616
		14	3·6461	7·4366	7·4367	10·9650	13·3315	13·3965	16·7376	6·7377	21·4518
	0·20	4	3·2087	16·7145	16·9462	16·9462	17·9005	18·0301	18·0301	19·6501	19·8229
		6	2·6635	5·1493	5·1493	7·0388	8·1667	8·3912	16·6452	17·1009	17·1009
		8	2·6395	4·6028	4·6028	6·1877	7·0794	7·2226	9·2421	9·2421	11·6094
		10	2·6393	4·5933	4·5933	6·1233	7·0096	7·1593	8·3282	8·3282	9·9343
		12	2·6392	4·5931	4·5931	6·1226	7·0085	7·1564	8·2813	8·2813	9·8241
		13	2·6392	4·5931	4·5931	6·1226	7·0084	7·1564	8·2799	8·2799	9·8211
		14	2·6392	4·5931	4·5931	6·1226	7·0084	7·1564	8·2799	8·2799	9·8210

TABLE 2

Comparison studies of frequency parameter, $\lambda = (\omega b^2/\pi^2)\sqrt{\rho t/D}$, *for thin square plate with four edges elastically restrained* (EEEE *plate*, $a/b = 1$ *and* $t/b = 0{\cdot}001$).

			Mode sequence								
S_w	S_ϕ	Sources	1	2	3	4	5	6	7	8	9
8	2	Present	0·5537	0·9605	0·9605	1·7720	2·7898	3·0169	3·9790	3·9790	6·7436
		Gorman [9]	0·5536	0·9605	0·9605	1·772	2·790	3·017	3·979	3·979	6·744
1176	98	Present	3·1006	5·6256	5·6256	7·5669	8·4857	8·8481	10·2436	10·2436	12·4474
		Gorman [9]	3·100	5·625	5·625	7·567	8·487	8·847	10·24	10·24	12·45
10^8	0	Present	2·0000	4·9996	4·9998	7·9996	9·9997	9·9997	12·9993	12·9994	16·9996
		Leissa [2]	2·00000	5·00000	5·00000	8·00000	10·0000	10·0000	13·0000	13·0000	17·0000
10^8	10^2	Present	3·5128	7·1716	7·1716	10·5832	12·8698	12·9297	16·1547	16·1547	20·6218
		Grossi and Bhat [13]	3·5137	–	–	–	–	–	–	–	–
10^8	10^8	Present	3·6461	7·4366	7·4366	10·9650	13·3315	13·3965	16·7376	16·7377	21·4518
		Leissa [2]	3·6468	7·4383	7·4383	10·970	13·338	13·399	–	–	–

$$\mathbf{K}_{de} = D\int_{\bar{A}} \left(v\,\frac{\partial \boldsymbol{\psi}_x}{\partial \xi}\frac{\partial \boldsymbol{\psi}_y^{\mathrm{T}}}{\partial \eta} + \frac{1-v}{2}\frac{\partial \boldsymbol{\psi}_x}{\partial \eta}\frac{\partial \boldsymbol{\psi}_y^{\mathrm{T}}}{\partial \xi} \right) \mathrm{d}\bar{A}, \tag{17e}$$

$$\mathbf{K}_{ee} = \frac{D}{ab}\int_{\bar{A}} \left[a^2\,\frac{\partial \boldsymbol{\psi}_y}{\partial \eta}\frac{\partial \boldsymbol{\psi}_y^{\mathrm{T}}}{\partial \eta} + \frac{(1-v)b^2}{2}\frac{\partial \boldsymbol{\psi}_y}{\partial \xi}\frac{\partial \boldsymbol{\psi}_y^{\mathrm{T}}}{\partial \xi} + a^2b^2\kappa G t \boldsymbol{\psi}_y \boldsymbol{\psi}_y^{\mathrm{T}} \right] \mathrm{d}\bar{A}, \tag{17f}$$

and the submatrices of $\mathbf{M}$ are given by

$$\mathbf{M}_{cc} = ab\rho t\int_{\bar{A}} \boldsymbol{\phi}\boldsymbol{\phi}^{\mathrm{T}}\,\mathrm{d}\bar{A}, \qquad \mathbf{M}_{dd} = \tfrac{1}{12}ab\rho t^3\int_{\bar{A}} \boldsymbol{\psi}_x\boldsymbol{\psi}_x^{\mathrm{T}}\,\mathrm{d}\bar{A}, \tag{18a, b}$$

$$\mathbf{M}_{ee} = \tfrac{1}{12}ab\rho t^3\int_{\bar{A}} \boldsymbol{\psi}_y\boldsymbol{\psi}_y^{\mathrm{T}}\,\mathrm{d}\bar{A}, \qquad \mathbf{M}_{cd} = \mathbf{M}_{ce} = \mathbf{M}_{de} = 0 \tag{18,c d}$$

The submatrices of $\mathbf{K}_s$ are given by

$$\mathbf{K}_{scc} = \int_{-1/2}^{1/2} k_w\{\delta_1[\boldsymbol{\phi}\boldsymbol{\phi}^{\mathrm{T}}]|_{\eta=-1/2} + \delta_2[\boldsymbol{\phi}\boldsymbol{\phi}^{\mathrm{T}}]|_{\eta=1/2}\}a\,\mathrm{d}\xi + \int_{-1/2}^{1/2} k_w\{\delta_3[\boldsymbol{\phi}\boldsymbol{\phi}^{\mathrm{T}}]|_{\xi=-1/2} + \delta_4[\boldsymbol{\phi}\boldsymbol{\phi}^{\mathrm{T}}]|_{\zeta=1/2}\}b\,\mathrm{d}\eta, \tag{19}$$

$$\mathbf{K}_{sdd} = \int_{-1/2}^{1/2} k_\phi\{\delta_7[\boldsymbol{\psi}_x\boldsymbol{\psi}_x^{\mathrm{T}}]|_{\xi=-1/2} + \delta_8[\boldsymbol{\psi}_x\boldsymbol{\psi}_x^{\mathrm{T}}]|_{\xi=1/2}\}b\,\mathrm{d}\eta, \tag{20}$$

TABLE 3

Comparison studies of frequency parameter, $\lambda = (\omega b^2/\pi)\sqrt{\rho t/D}$, for simply supported thick square plate with four edges elastically restrained against rotation (SSSS *plate*, $a/b = 1$ *and* $t/b = 0{\cdot}1$).

		Mode sequence					
S_ϕ	Sources	1	2	3	4	5	6
10^1	Present	2·6722	5·3657	5·3657	7·7021	9·2707	9·3212
	Chung *et al*· [14]	2·672	5·376	5·378	7·781	9·290	9·316
10^2	Present	3·1736	6·0706	6·0706	8·4997	10·0603	10·1671
	Chung *et al*· [14]	3·075	5·930	5·932	8·384	9·905	9·977
10^3	Present	3·2617	6·2090	6·2090	8·6650	10·2329	10·3518
	Chung *et al*· [14]	3·242	6·190	6·194	8·690	10·266	10·322

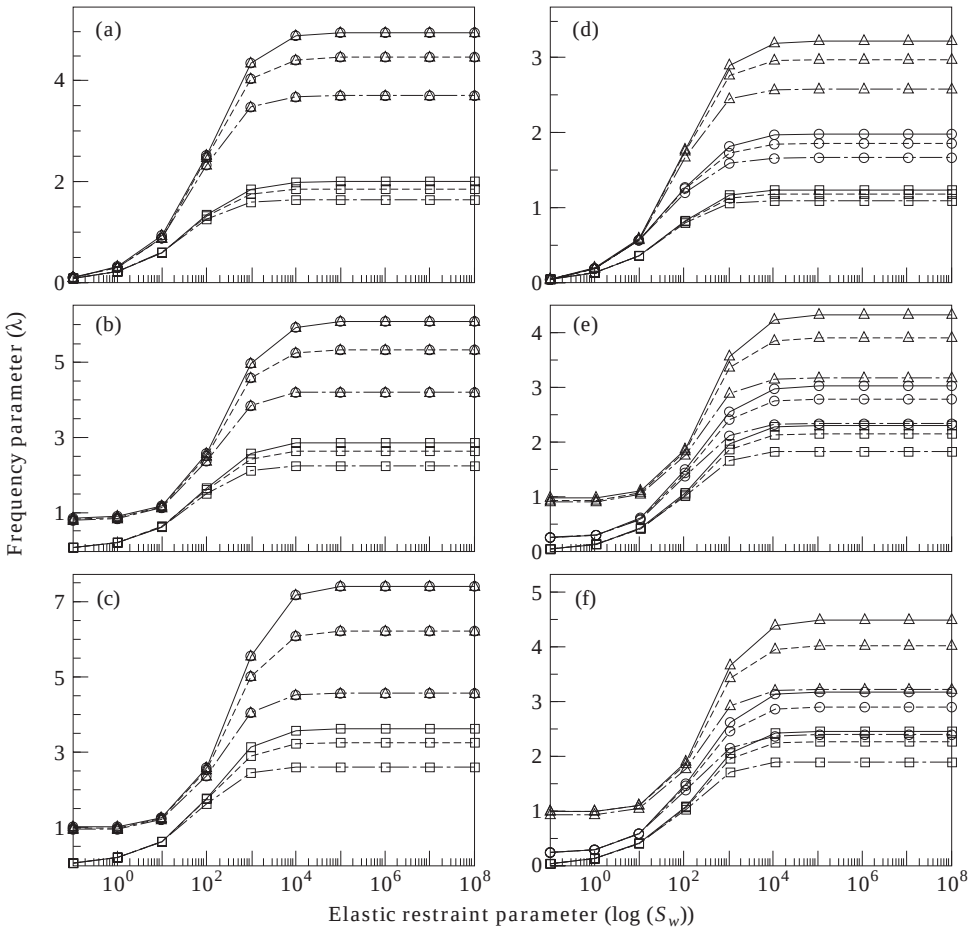

Figure 3. Frequency parameter, $\lambda = (\omega b^2/\pi^2)(\rho t/D)^{1/2}$ versus the elastic lateral edge restraint parameter, S_w, for rectangular Mindlin plate with EEEE edge conditions. Key: ——, t/b = 0·001; – – –, t/b = 0·1; –·–·–, t/b = 0·2; □, first mode; ○, second mode; △, third mode. a/b and S_ϕ values respectively are: (a) 1, 0; (b) 1, 10^2; (c) 1, 10^8; (d) 2, 0; (e) 2, 10^2; (f) 2, 10^8.

$$\mathbf{K}_{see} = \int_{-1/2}^{1/2} k_\phi \{\delta_5[\boldsymbol{\psi}_y \boldsymbol{\psi}_y^{\mathrm{T}}]|_{\eta=-1/2} + \delta_6[\boldsymbol{\psi}_y \boldsymbol{\psi}_y^{\mathrm{T}}]|_{\eta=1/2}\} a \, \mathrm{d}\xi, \tag{21}$$

$$\mathbf{K}_{scd} = \mathbf{K}_{sce} = \mathbf{K}_{sde} = 0. \tag{22}$$

The frequency parameters, $\lambda = (\omega b^2/\pi^2)\sqrt{\rho t/D}$, are obtained by solving the generalised eigenvalue problem defined by equation (15) using subroutine RSG in EISPACK.

3. RESULTS AND DISCUSSION

The completeness of the formulation is further furnished by numerical examples. Three examples of Mindlin plates have been considered: (1) all four edges elastically restrained (EEEE); (2) two opposite sides simply supported and the others elastically restrained (SESE); and (3) two opposite sides clamped and the others elastically restrained (CECE);

as shown in Figure 2. Note that the notation E is introduced to represent an edge with elastic restraints against both rotational and transverse displacements. The Poisson ratio has been fixed at 0·3 and shear correction factor κ has been taken as 5/6 throughout the study.

For generality and convenience, two non-dimensionalised elastic restraint parameters have been adopted in the following numerical analysis:

$$S_w = k_w b^3/D, \qquad S_\phi = k_\phi b/D. \tag{23, 24}$$

Before the numerical results are examined, it is appropriate to look at the results of some convergence and comparison studies. The convergence of the eigenvalue is firstly established by a numerical study as shown in Table 1. This convergence study considered a square Mindlin plate with four edges elastically restrained (EEEE plate, $S_w = S_\phi = 10^2$ and 10^8). The downward convergence of eigenvalue, which is the characteristic of the Ritz method, is clearly demonstrated. The existence of the upperbound eigenvalue is mainly due to the overestimation of plate stiffness by the Ritz procedure. A satisfactory numerical

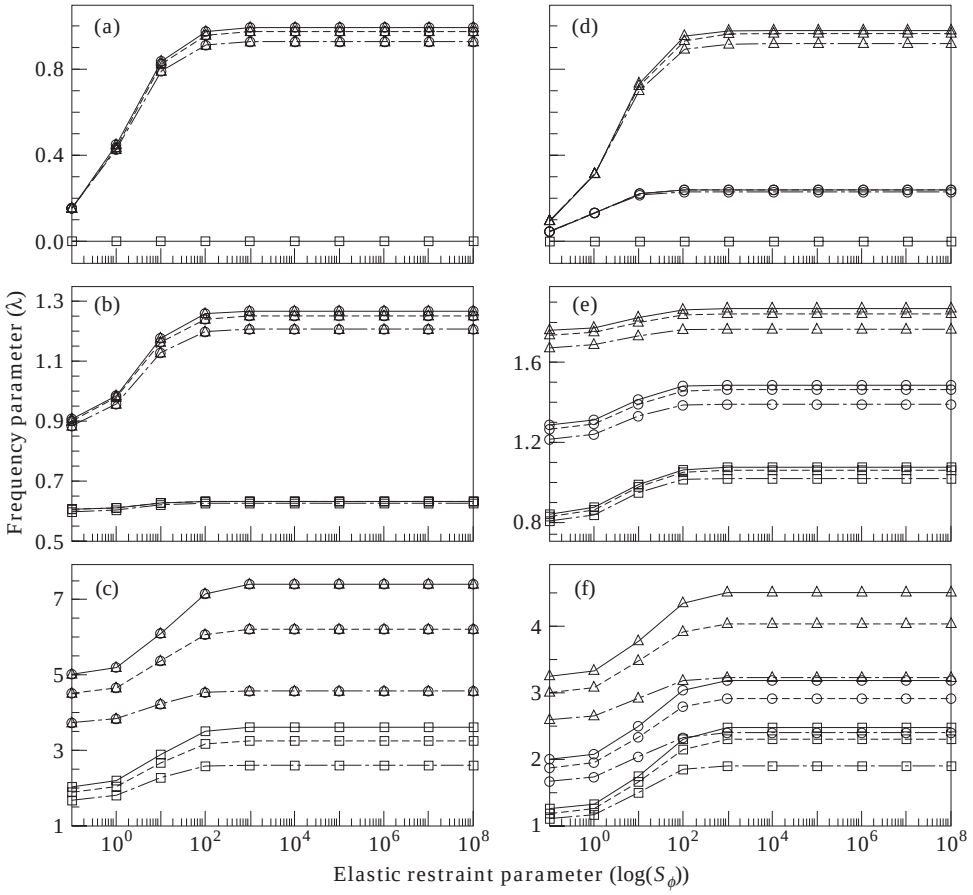

Figure 4. Frequency parameter, $\lambda = (\omega b^2/\pi^2)(\rho t/D)^{1/2}$ versus the elastic rotational edge restraint parameter, S_ϕ, for rectangular Mindlin plate with EEEE edge conditions. Key as for Figure 3. a/b and S_w values respectively are: (a) 1, 0; (b) 1, 10^2; (c) 1, 10^8; (d) 2, 0; (e) 2, 10^2; (f) 2, 10^8.

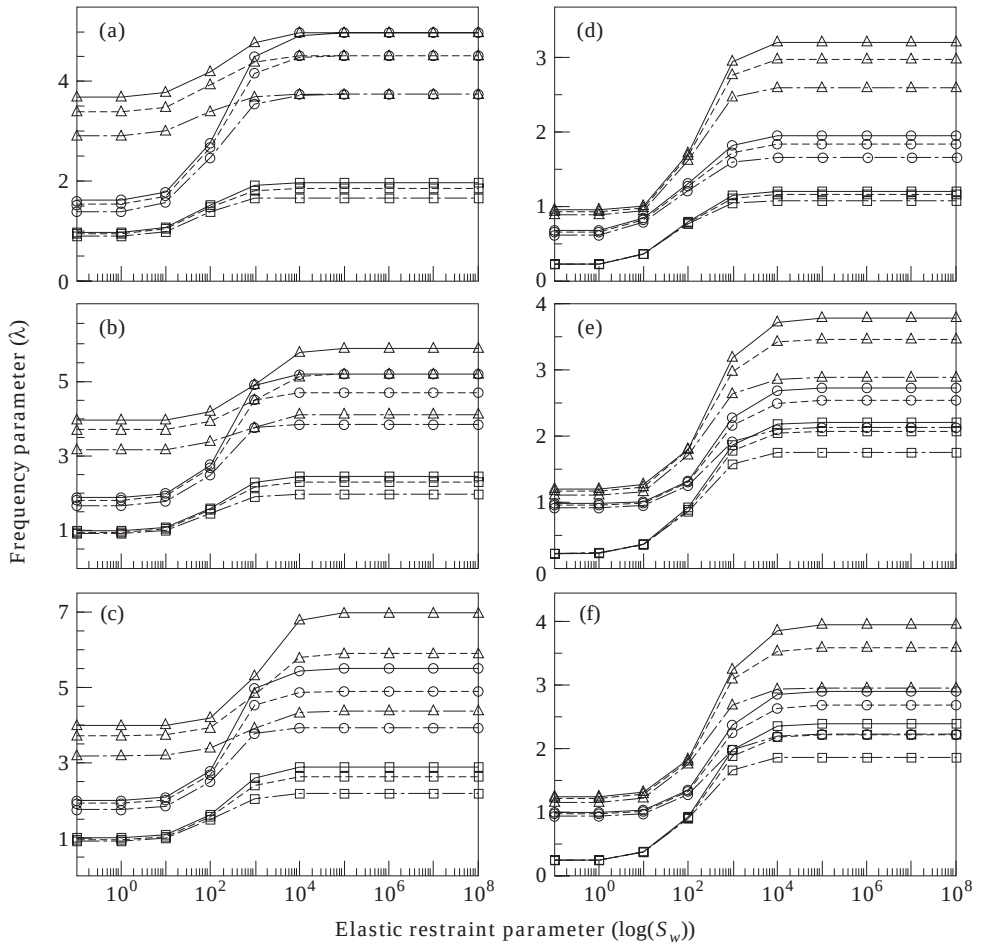

Figure 5. Frequency parameter, $\lambda = (\omega b^2/\pi^2)(\rho t/D)^{1/2}$ versus the elastic lateral edge restraint parameter, S_w, for rectangular Mindlin plate with SESE edge condtions. Key as for Figure 3.

accuracy can be achieved by employing a higher number of terms in the approximation of the trial functions.

The convergence study covered two plate thickness ratios $t/b = 0{\cdot}001$ (thin) and $0{\cdot}20$ (moderately thick). The number of degree of polynomials p_s used in the trial functions increases from 4 to 14 which is equivalent to changing the determinant size of the eigenvalue equation from 45×45 to 360×360. It is observed that a degree of polynomial $p_s = 12$, which is equivalent to a determinant size of 273×273, is sufficient to furnish convergent eigenvalues for plates with elastic restraint parameter $S_w = S_\phi = 10^2$, while $p_s = 14$ is required to generate a satisfactory convergence of eigenvalues for plates with elastic restraint parameter $S_w = S_\phi = 10^8$. Throughout this study, $p_s = 14$ has been used in all computations to ensure satisfactory convergence of eigenvalues for all cases.

Table 2 presents frequency parameters generated by the authors and by Leissa [2], Gorman [9] and Grossi and Bhat [13] for thin square plates ($t/b = 0{\cdot}001$) with all edges elastically restrained against transverse and rotational displacements (EEEE plate). Excellent agreement has been achieved between the present results

and the results in references [2], [9] and [13]. Frequency parameters are presented in Table 3 for simply supported thick square plates ($t/b = 0{\cdot}1$) with edges elastically restrained against rotation. The results obtained using the present method are in good agreement with the results reported by Chung *et al*. [14].

Having confirmed the proposed method by the foregoing convergence and comparison studies, this method has been applied to generate frequency responses for the three example problems (see Figure 2) for two plate aspect ratios, $a/b = 1{\cdot}0$ and $2{\cdot}0$. The results are shown in Figures 3–8. The elastic restraint parameter (S_w or S_ϕ) varies from 10^{-1} (a very small restraint) to 10^8 (approaches infinite restraint) while the thickness ratio t/b ranges from 0·001 (a thin plate) to 0·20 (a moderately thick plate). Thus, the coverage of the results is relatively thorough and complete because the results extend from narrow to wide, and thin to thick plates. The effects of t/b, a/b and S_w (or S_ϕ) upon the vibratory responses are evident from Figures 3–8.

The frequency parameters λ for the first three modes are presented in: (1) Figures 3 and 4 for the EEEE plate (Case I in Figure 2); (2) (Figures 5 and 6 for the SESE plate (Case

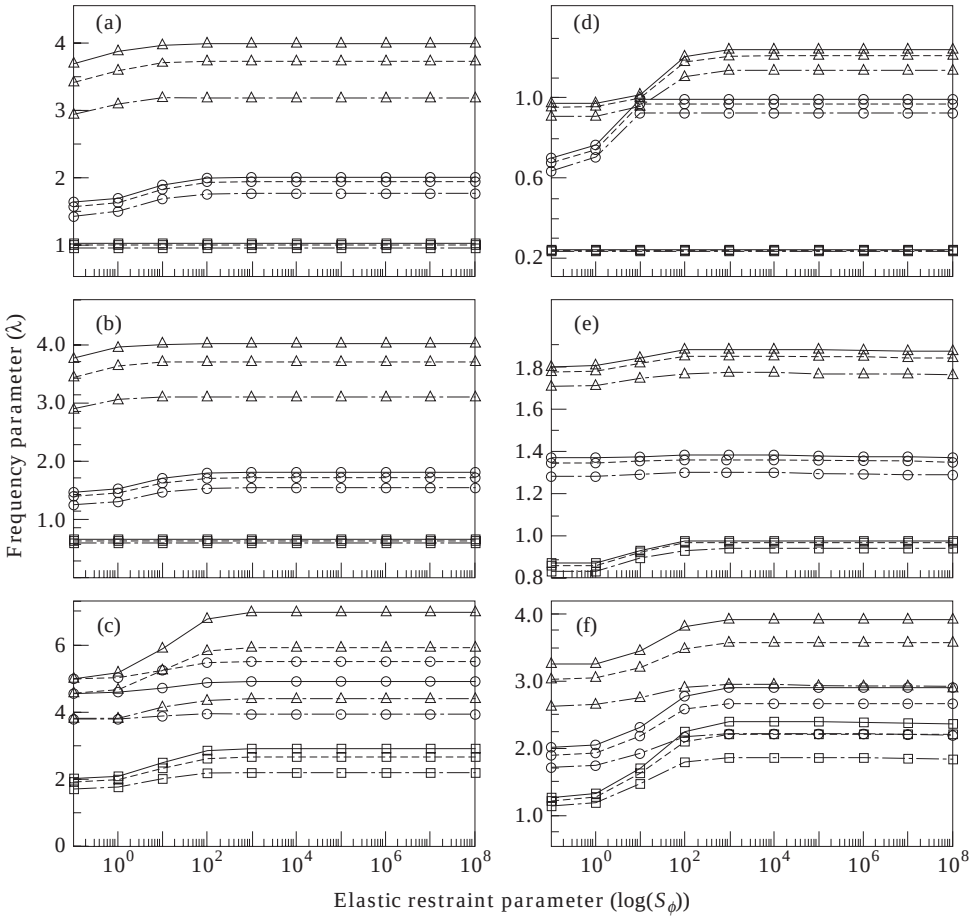

Figure 6. Frequency parameter, $\lambda = (\omega b^2/\pi^2)(\rho t/D)^{1/2}$ versus the elastic rotational edge restraint parameter, S_ϕ, for rectangular Mindlin plate with SESE edge conditions. Key as for Figure 4.

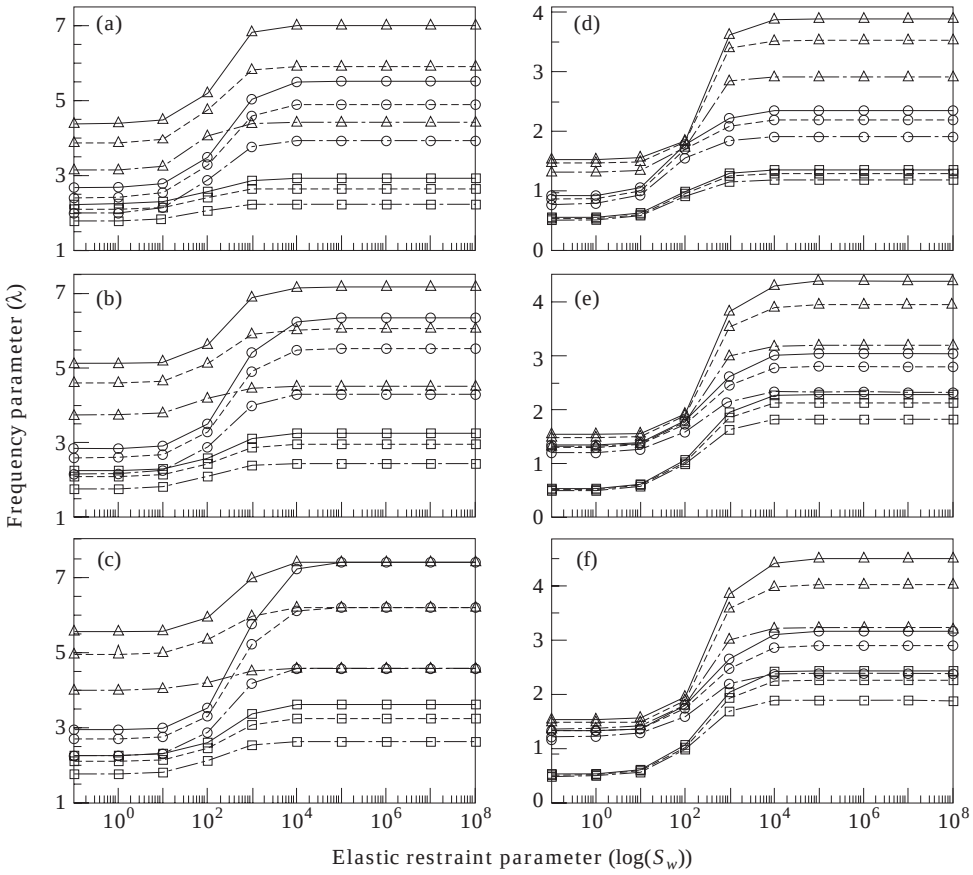

Figure 7. Frequency parameter, $\lambda = (\omega b^2/\pi^2)(\rho t/D)^{1/2}$ versus the elastic lateral edge restraint parameter, S_w, for rectangular Mindlin plate with CECE edge conditions. Key as for Figure 4.

II in Figure 2); and (3) Figures 7 and 8 for the CECE plate (Case III in Figure 2) by varying the elastic restraint parameters. In general, it is observed that the frequency parameter beyond a certain large value (say 10^4), the rate at which the frequency parameter approaches the upper limit is relatively slow. This is almost certainly due to the nature of the stiff elastic restraints which are approaching the classical supporting edge conditions of the plate.

It is further observed that the frequency parameter decreases as the plate thickness ratio increases. This confirms that the frequency parameter of a thicker plate is lower than that of a thinner plate due to the effects of transverse shear deformation and rotary inertia. These effects are more pronounced for plates with larger thickness ratios and vibrating in higher modes.

It is interesting that for some examples (see Figures 5 and 8), mode crossings are observed as the elastic restraint parameters approach certain values ($S_w > 10^4$ or $S_w > 10^5$ in Figure 5(a)). It is further noted that the fundamental modes for cases 4(a) and 4(d) in Figure 4 are the rigid body mode which has a zero natural frequency parameter.

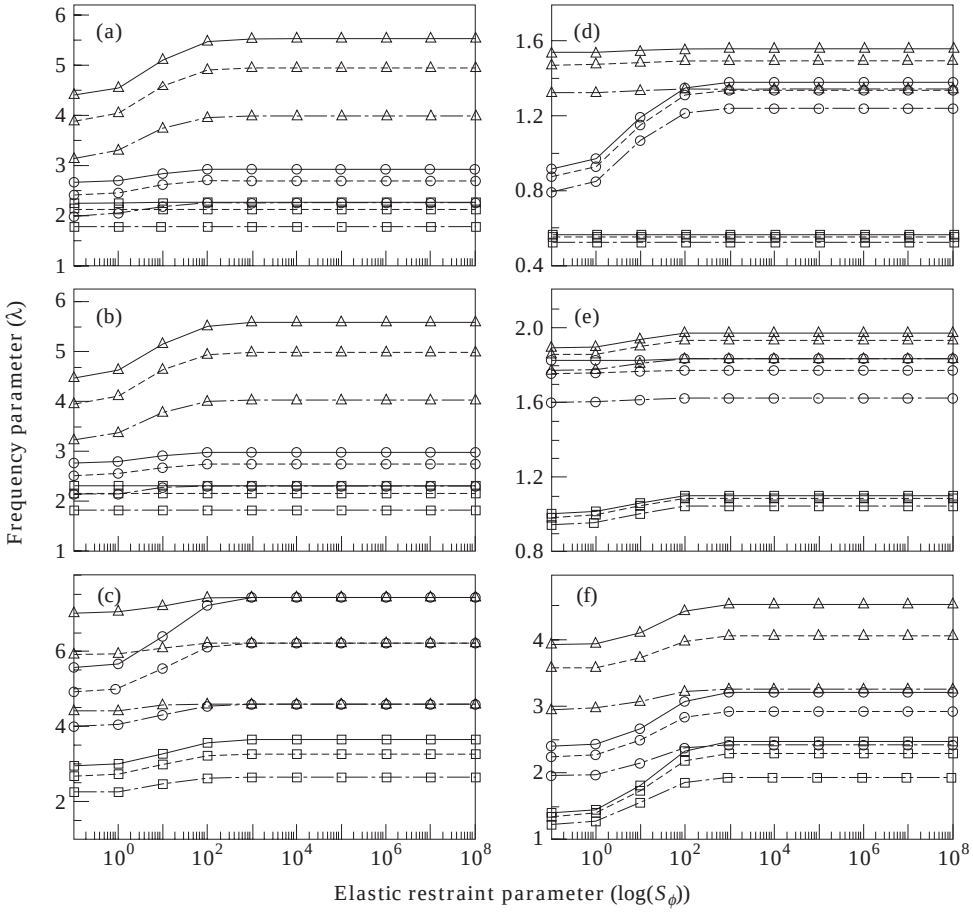

Figure 8. Frequency parameter, $\lambda = (\omega b^2/\pi^2)(\rho t/D)^{1/2}$ versus the elastic rotational edge restraint parameter, S_ϕ, for rectangular Mindlin plate with CECE edge conditions. Key as for Figure 4.

4. CONCLUDING REMARKS

This paper presents, to the authors' knowledge, the first known vibration analysis of thick rectangular plates with edges elastically restrained against transverse and rotational displacements. The rotational and transverse elastic restraints may be used to simulate the actual boundary conditions of the plates. Three example problems are presented to illustrate the applicability of the method. The present method is, however, a very general approximate technique which is able to provide vibration solutions for plates with any combination of boundary conditions and elastically restrained edges. The results shown in the design charts may be useful to engineers by providing them with direct frequency parameters if their problems fall within the range for which results are plotted. It is expected that the data presented in this paper will serve an important role in providing other researchers with reference values with which to compare their results.

REFERENCES

1. A. W. Leissa 1969 *Vibration of Plates* (NASA SP-160). Washington, D.C.: U.S. Government Printing Office.

2. A. W. Leissa 1973 *Journal of Sound and Vibration* **31**, 257–293. The free vibration of rectangular plates.
3. C. S. Kim and S. M. Dickinson 1987 *Journal of Sound and Vibration* **117**, 249–261. The flexural vibration of rectangular plates with point supports.
4. D. J. Gorman 1982 *Free Vibration Analysis of Rectangular Plates*. New York: Elsevier North Holland.
5. P. A. A. Laura, R. O. Grossi and S. R. Soni 1979 *Journal of Sound and Vibration* **62**, 493–503. Free vibrations of a rectangular plate of variable thickness elastically restrained against rotation along three edges and free on the fourth edge.
6. P. A. A. Laura, R. O. Grossi and G. I. Carneiro 1979 *Journal of Sound and Vibration* **63**, 499–505. Transverse vibration of rectangular plates with thickness varying in two directions and with edges elastically restrained against rotation.
7. P. A. A. Laura and R. O. Gross 1981 *Journal of Sound and Vibration* **75**, 101–107. Transverse vibration of rectangular plates with edges elastically restrained against rotation and translation.
8. P. A. A. Laura and R. H. Gutierrez 1981 *Journal of Sound and Vibration* **78**, 139–144. A note on transverse vibrations of stiffened rectangular plates with edges elastically restrained against rotation.
9. D. J. Gorman 1989 *ASME Journal of Applied Mechanics* **56**, 893–899. A comprehensive study of the free vibration of rectangular plates resting on symmetrically distributed uniform elastic edge supports.
10. D. J. Gorman 1990 *Journal of Sound and Vibration* **139**, 325–335. A general solution for the free vibration of rectangular plates resting on uniform elastic edge supports.
11. T. Mizusawa and T. Kajita 1986 *Computers and Structures* **22**, 987–994. Vibration and buckling of skew plates with edges elastically restrained against rotation.
12. M. Mukhopadhyay 1979 *Journal of Sound and Vibration* **67**, 459–468. Free vibration of rectangular plates with edges having different degrees of rotational restraint.
13. R. O. Grossi and R. B. Bhat 1995 *Journal of Sound and Vibration* **185**, 335–343. Natural frequencies of edge restrained tapered rectangular plates.
14. J. H. Chung, T. Y. Chung and K. C. Kim 1993 *Journal of Sound and Vibration* **163**, 151–163. Vibration analysis of orthotropic Mindlin plates with edges elastically restrained against rotation.
15. W. H. Liu and C.-C. Huang 1987 *Journal of Sound and Vibration* **119**, 177–182. Free vibration of a rectangular plate with elastically restrained and free edges.
16. H. Kobayashi and K. Sonada 1991 *Journal of Sound and Vibration* **146**, 323–327. Vibration and buckling of tapered rectangular plates with two opposite edges simply supported, other two edges elastically restrained against rotation.
17. M. Mukhopadhyay 1989 *Computers and Structures* **32**, 341–346. Vibration and stability analysis of rectangular plates.
18. G. B. Warburton and S. L. Edney 1984 *Journal of Sound and Vibration* **95**, 537–552. Vibration of rectangular plates with elastic restrained edges.
19. A. W. Leissa 1977 *The Shock and Vibration Digest* **9**, 13–24. Recent research in plate vibrations: classical theory.
20. A. W. Leissa 1981 *The Shock and Vibration Digest* **13**, 11–22. Plate vibration research, 1976–1980: classical theory.
21. A. W. Leissa 1987 *The Shock and Vibration Digest* **19**, 11–18. Recent research in plate vibrations: 1981–1985: Part I. Classical theory.
22. R. D. Mindlin 1951 *ASME Journal of Applied Mechanics* **18**, 31–38. Influence of rotary inertia and shear in flexural motion of isotropic, elastic plates.
23. K. M. Liew 1993 *International Journal of Solids and Structures* **30**, 337–347. Treatment of over-restrained boundaries for doubly connected plates of arbitrary shape in vibration analysis.
24. S. Kitipornchai, Y. Xiang, C. M. Wang and K. M. Liew 1993 *International Journal for Numerical Methods in Engineering* **36**, 1299–1310. Buckling of thick skew plates.
25. K. M. Liew, Y. Xiang, C. M. Wang and S. Kitipornchai 1993 *Computer Methods in Applied Mechanics and Engineering* **110**, 301–315. Flexural vibration of shear deformable circular and annular plates on ring supports.